The angular power spectrum of the Galactic radio background

PHILIPP MERTSCH[1], SUBIR SARKAR[2]

[1] *Kavli Institute for Particle Astrophysics & Cosmology, 2575 Sand Hill Road, M/S 29, Menlo Park, CA 94025, USA*
[2] *Rudolf Peierls Centre for Theoretical Physics, University of Oxford, 1 Keble Road, Oxford OX1 3NP, UK*

pmertsch@stanford.edu

Abstract: We study the Galactic radio background produced by synchrotron emission of cosmic ray electrons in Galactic magnetic fields. The angular power spectrum of all-sky maps contains contributions from physical processes on a variety of scales, including the variation of emissivity on large (kpc) scales and the small-scale turbulence in the interstellar medium. Previous studies have focussed on one scale or the other but have not provided a self-consistent picture valid on all scales. We show that the angular power spectrum in the multipole range $l \sim 10-100$ has a deficit with respect to observations at 408 MHz and suggest that the shells of old supernova remnants (like the well-known 'radio loops') can provide the missing power. We model the emissivity from individual shells and find that the Galactic population of $\mathscr{O}(1000)$ shells naturally provides the missing power and brings the modelled angular power spectrum into agreement with the observed one. This has important implications for studies of the cosmic microwave background, in particular B-mode polarisation.

Keywords: Galactic radio background, CMB foregrounds, cosmic ray electrons

1 Introduction

The sky at radio wavelengths is dominated by diffuse emission from the Galaxy. Besides free-free emission, i.e. bremsstrahlung of non-thermal electrons on interstellar gas, it is mostly synchrotron emission of high-energy electrons gyrating in interstellar magnetic fields. For field strengths of a few μG, the emission between tens of MHz and a few GHz is produced by cosmic ray (CR) electrons of $\mathscr{O}(100)$ MeV to $\mathscr{O}(10)$ GeV. These electrons are most likely accelerated by diffusive shock acceleration in supernova remnants (SNRs). The transport of electrons of these energies is believed to be dominated by diffusion through scattering on turbulent magnetic fields in the interstellar medium. At the highest energies, not only synchrotron radiation but also inverse Compton scattering on the interstellar radiation fields leads to rapid energy loss. Consequently, the details of both the source distribution and the diffusion model are encoded in the radio spectrum and its angular distribution. Therefore, the radio background contains valuable information that is crucial, for example, for unravelling cosmic ray backgrounds in searches for dark matter annihilation signals.

The diffuse Galactic radio background also constitutes a *foreground* for studies of cosmic microwave background (CMB) anisotropies [1], both in temperature and in polarisation. Only around 70 GHz and at high Galactic latitudes do the CMB temperature anisotropies dominate over the Galactic foregrounds [2]. For the elusive B-mode, a crucial diagnostic of primordial inflation, the expected CMB signal is smaller than the foregrounds by over an order of magnitude. It is obvious that a detailed understanding of the foregrounds is crucial for detecting the B-mode polarisation [3, 4, 5] and also for fully harvesting the physics potential of the temperature anisotropies.

Although we are far from a full understanding of the strength and structure of the Galactic magnetic fields, it is conventional to distinguish between a large-scale ordered component that varies on kiloparsec scales and a small-scale turbulent component. The large-scale field is believed to align with the spiral arms and field strengths of a few μG have been inferred from the rotation measures of Galactic and extragalactic radio sources. The small-scale component is due to energy injected on large scales by Galactic winds and supernova explosions that is cascading down to smaller scales. Both observations of interplanetary plasmas and numerical simulations point at turbulence satisfying Kolmogorov phenomenology, i.e. the 3D power spectrum $P(k) \propto k^{-11/3}$. Such small-scale correlations in the magnetic fields are reflected [6, 7, 8, 9] in the angular correlations of the synchrotron sky map $J(\theta,\phi)$, more specifically in the angular power spectrum (APS):

$$\mathscr{C}_l \equiv \frac{1}{2l+1} \sum_{m=-l}^{l} |a_{lm}|^2 \ \text{with}\ a_{lm} = \int \mathrm{d}\Omega\, Y^*_{lm}(\theta,\phi) J(\theta,\phi),$$

where $Y_{lm}(\theta,\phi)$ are the spherical harmonic functions. This definition of the APS is equivalent to the Legendre transform of the two-point angular correlation function for a (statistically) isotropic random field. For the quoted power law in 3D, the APS would be a broken power law with $\mathscr{C}_l \propto l^{-1}$ below and $\mathscr{C}_l \propto l^{-11/3}$ above a critical multipole $l_{\mathrm{cr}} \sim L/R$, where L is the 'outer scale' of turbulence and R is the column length of the turbulent medium.

Modelling of the Galactic radio background so far has focussed on either large or small scales. On the largest scales, the propagation of electrons [10, 11, 12, 13] and the magnetic fields [14, 15, 16, 17] have been modelled in some detail, using information on the diffusion model parameters from local observations of nuclear cosmic rays. While a lot of effort has been made to reproduce the overall spectrum at intermediate and high latitudes, angular profiles are not always well reproduced by the simulations. This is partly due to the presence of structures on intermediate scales, like the 'radio loops' which extend over large regions of the sky but are ignored in such simulations. On the smallest scales, the APS has been fitted with a power law in attempts to determine both the power law index and the outer scale of the underlying turbulence. However, structure on larger scales is usually ignored which leads to an unrealistically small height for the comic ray halo [18].

Here, we unify these approaches focussing on the APS of the Galactic radio background by modelling both the large-scale emissivity *and* the small-scale turbulence. Somewhat unexpectedly, we find that even after accounting for free-free emission and unsubtracted point-sources, the observed APS cannot be reproduced as the model lacks power at intermediate scales $l \sim 10$ to 100. We suggest that the structures at intermediate scales could be the shells of old SNRs, like those observed in the radio sky as giant arcs or 'radio loops'. We construct a simple model of the emission from these shells, and their APS, that enables us to close the gap in the total APS, making only moderate assumptions on the free parameters — mainly the number of these shells (which fixes the normalisation of this new component).

For our study we constrain ourselves to the well-known 408 MHz all-sky survey [19] which has been cleaned of scanning artefacts and known point sources. To compute the APS, we have used the `HEALPix` suite [20].

2 Modelling the angular power spectrum

2.1 Synchrotron emissivity on large scales

We employ the `GALPROP` code [21] to compute the propagation of CR electrons and the synchrotron sky at radio wavelengths. The code is based on a numerical integration of the CR transport equation and can take into account diffusion, convection, reacceleration as well as energy losses through synchrotron emission and inverse compton scattering. It was shown that the source spectrum must posses a spectral break around a few GeV in order not to overproduce the radio spectrum at intermediate to high Galactic latitudes [22]. We therefore adopt a power law index of 1.6 below 4 GV, and 2.5 above. The sources are assumed to follow the radial distribution of pulsars as parametrised in [23]. For the spatial diffusion coefficient $D_{xx} = D_0(\mathscr{R}/4\,\mathrm{GV})^{\delta}$, we adopt the values determined from a Bayesian analysis of locally measured nuclear cosmic rays [24], $D_0 = 3.4 \times 10^{28}\,\mathrm{cm\,s}^{-1}$ and $\delta = 0.5$, as well as $z_{\max} = 4\,\mathrm{kpc}$ for the height of the cylindrical cosmic ray halo. We assume no convection (for simplicity) and no reacceleration. For the turbulent magnetic field (the regular component is subdominant, so we ignore it for simplicity), we have adopted an exponential dependence on galacto-centric radius r and distance from the disk z, $B_{\mathrm{rms}} \propto \exp[-r/\rho - z/\xi]$ with $\rho = 100\,\mathrm{kpc}$ and $\xi = 4\,\mathrm{kpc}$. The normalisation of the field is fixed by requiring the low multipoles (up to $l \sim 20$) to reproduce the observed dipole.

2.2 Synchrotron emissivity on small scales

The adopted broken power law for the APS on small scales has been derived for a statistically isotropic turbulent medium, however the Galactic radio halo is anisotropic, both because of the source distribution in the Galactic disk, and the off-centre position of the Solar system. While is is conceivable that the power law pertains even in a (statistically) anisotropic setup like the Galactic radio halo, it is not clear how the APS at small scales blends into the APS at large scales. We have therefore numerically computed the synchrotron sky by preparing an isotropic Gaussian random field with outer scale $L \approx 400\,\mathrm{pc}$ that we then dressed with the distribution of emissivity on large-scales as calculated for Sec. 2.1 and projected along the line of sight. It turns out that the contribution on top of the large-scale component is very small (compare the orange and red lines in Fig. 1), which can be understand using simple arguments comparing the power in the monopole with the total power contained in larger multipoles. (For details, see our paper [25]).

2.3 Free-free emission

We employ a template to model the free-free emission that has been obtained by a maximum entropy method applied to WMAP data [26]. Although far from perfect, it has been shown to be more reliable than Hα maps which suffer from strong absorption around the Galactic plane.

2.4 Unsubtracted point sources

Although care has been exercised in removing the known sources from the 408 MHz sky map, only sources above a certain flux threshold can be subtracted off. For example, it has been estimated [27] that for Galactic latitudes $|b| \geq 45°$, all sources with a peak flux of 6.4 Jy and above have been removed. To account for the contribution of unremoved sources, we model their APS directly as shot noise, i.e. $\mathscr{C}_l \sim$ const. and fix the amplitude to match the observed APS at the largest multipoles considered here, i.e. $l \sim 200$.

2.5 Old shells of SNRs

We will see in the next section that the sum of the components considered above misses power on intermediate scales, $l \sim 10 - 100$ (corresponding to angular scales of $20° \to 2°$). This is the range of scales that is usually ignored in the computation of synchrotron spectra and angular profiles of radio maps. However, inspection of radio maps (especially in polarised intensity) reveals coherent ring- and arch-like structures, spanning between a few to a few tens of degrees — the 'radio loops' [28, 29]. These structures are believed to be the shells of old supernova remnants (SNRs) that have expanded over $\mathscr{O}(10^5)$ yr up to radii of $\mathscr{O}(100)$ pc [30]. Although the shock acceleration of particles is likely to have stalled in this radiative phase, the compression factor η can be very large such that the interstellar magnetic field gets efficiently compressed. The electrons are simultaneously compressed *and* betatron accelerated such that the synchrotron emissivity of the shells is strongly boosted. In line with the benchmark age above, we adopt a typical radius of 200 pc.

We approximate the emissivity of an old SNR by a thin shell of constant emissivity and relate their spectrum to the compressed and betatron accelerated emissivity of the ambient interstellar medium. The sky map from a single shell then factorises into an angular and a frequency part. The spherical harmonics coefficient a^i_{lm} for a shell i at position $\vec{r}_i$ in the Galactic disk, seen at Galactic longitude and latitude (ℓ_i, b_i), then computes as

$$a^i_{lm} = \varepsilon_i(\nu) Y^*_{lm}\left(\frac{\pi}{2} - b_i, -\ell_i\right) \int_{-1}^{1} \mathrm{d}z' P_l(z') g(z') \,. \qquad (1)$$

where ε_i

$$\varepsilon_i(\nu, \eta B) = \sqrt{\frac{8}{3}}\,\eta\, \varepsilon_{\mathrm{ISM}}\left(\frac{3\nu}{2\eta^2}, B\right) , \qquad (2)$$

is the ISM emissivity $\varepsilon_{\mathrm{ISM}}$, rescaled to take into account the compression of the magnetic fields and betatron acceleration, and where $g(\cos\psi)$ is the angular profile of the shell, i.e. the line of sight integral as a function of angular distance ψ from the centre of the shell. $P_l(z)$ is the Legendre polynomial of degree l.

For the benchmark age $t = 10^5$ yr, and with a Galactic supernova rate of $\sim 10^{-2}\,\mathrm{yr}^{-1}$, we expect ~ 1000 old SNRs to contribute to the APS. Note that this number is larger than the number of SNRs identified in radio catalogues [31] since the majority of the old shells can be difficult to identify if they are deep in the Galactic disk [32]. We add up the a^i_{lm} for this Galactic population of shells and add those for the four local radio loops with the positions as in [28] to compute the APS. (For details, see [25]).

3 Results

In Fig. 1 we show the APS for the different components contributing to the Galactic radio background: the contribution from the smooth variation of synchrotron emissivity (red line), both large- and small-scale (turbulent) contributions (orange line), thermal bremsstrahlung (yellow line), unsubtracted point-sources (grey line) and the sum of all components (blue line), compared with the 408 MHz all-sky survey (black line). It can be seen that the large-scale variation of the ISM emissivity dominates as expected on the largest angular scales (up to $l \sim 20$), while at the smallest angular scales ($l \gtrsim 20$) most of the power is contributed by the variation of the free-free emission. At intermediate scales ($l \sim 10-100$), however, there is clearly a lack of power in the computed APS with respect to the one of the 408 MHz survey, up to 50 % around $l \sim 40$. (This is conservative since with the adopted normalisation, the multipoles $l \lesssim 10$ are overproduced.) Although for the large-scale emission (see Sec. 2.1) some power can be moved to higher multipoles by modifying the propagation parameters, this would dramatically reduce the power in the dipole and quadrupole, leading to a strong deficit. Finally, we note that the small-scale variations of emission (ISM turbulence) do lead to the expected power law $\propto l^{-11/3}$ but are always subdominant.

In Fig. 2 we now include the APS of the Galactic population of old SNRs (green line) and of the four local radio loops (green-blue line). The $\mathcal{O}(1000)$ shells give a very regular APS and contribute between $l \sim 10$ and 80. The APS of the nearby four local loops has a much more irregular structure and contributes at larger angular scales, mostly below $l \sim 50$. Adding their contribution to the other components (we renormalise the large/small-scale ISM contribution to allow for the the additional components), the agreement of the total APS with that of the Haslam 408 MHz all-sky survey is excellent, with the residuals being 10% at most. The remaining differences for $l \gtrsim 100$ are probably due to the less-than-perfect free-free template.

4 Conclusions

We have provided a new model for the diffuse, Galactic synchrotron background, directly modelling and fitting to the APS, as opposed to full-sky maps. We find that the components usually considered, i.e. large and small-scale variations of the ISM emissivity, free-free emission and unsubtracted point sources, leads to a deficit with respect to observations. Adding in the expected (and so far ignored) contributions from the shells of old SNRs (only *locally* observable in sky maps as the radio loops) provides the additional power on intermediate scales. We believe that this approach allows for direct foreground cleaning in the APS (as opposed to template subtraction on sky maps) and can easily be applied to polarised emission as well.

Acknowledgment: SS would like to thank the Niels Bohr International Academy, Copenhagen for hospitality as a Visiting Professor. PM thanks Prof Pavel Naselsky of the 'Discovery Center', Niels Bohr Institute for support and for very useful discussions. This work was supported in part by the Department of Energy contract DE-AC02-76SF00515 and the KIPAC Kavli Fellowship made possible by The Kavli Foundation.

References

[1] W. Hu and S. Dodelson, *Ann. Rev. Astron. Astrophys.* **40** (2002) 171, [astro-ph/0110414].
[2] **WMAP** Collaboration, C. Bennett *et. al.*, *Astrophys. J.Suppl.* **148** (2003) 97, [astro-ph/0302208].
[3] J. Dunkley, A. Amblard, C. Baccigalupi, M. Betoule, D. Chuss, *et. al.*, *AIP Conf. Proc.* **1141** (2009) 222, [arXiv:0811.3915].
[4] **COrE** Collaboration, F. Bouchet *et. al.*, arXiv:1102.2181.
[5] J. Delabrouille, M. Betoule, J.-B. Melin, M.-A. Miville-Deschenes, J. Gonzalez-Nuevo, *et. al.*, arXiv:1207.3675.
[6] A. V. Chepurnov, *Astron. Astrophys. Trans.* **17:4** (1998) 281.
[7] J. Cho and A. Lazarian, *Astrophys. J.* **575** (2002) L63, [astro-ph/0205284].
[8] J. Cho and A. Lazarian, *Astrophys. J.* **720** (2010) 1181, [arXiv:1007.3740].
[9] A. Lazarian and D. Pogosyan, *Astrophys. J.* **747** (2012) 5, [arXiv:1105.4617].
[10] E. Orlando, A. Strong, I. Moskalenko, T. Porter, G. Johannesson, *et. al.*, *Proc. 31st International Cosmic Ray Conference, Lodz* (2009) [arXiv:0907.0553].
[11] T. R. Jaffe, A. J. Banday, J. P. Leahy, S. Leach, and A. W. Strong, *MNRAS* **416** (2011) 1152, [arXiv:1105.5885].
[12] T. Bringmann, F. Donato, and R. A. Lineros, *JCAP* **1201** (2012) 049, [arXiv:1106.4821].
[13] T. Jaffe, K. Ferriere, A. Banday, A. Strong, E. Orlando, *et. al.*, arXiv:1302.0143.
[14] X. Sun, W. Reich, A. Waelkens, and T. Enslin, *Astron. Astrophys.* **477** (2008) 573, [arXiv:0711.1572].
[15] X. Sun and W. Reich, *Res. Astron. Astrophys.* **10** (2010) 1287, [arXiv:1010.4394].
[16] L. Fauvet, J. Macias-Perez, J. Aumont, F. Desert, T. Jaffe, *et. al.*, *Astron. Astrophys.* **526** (2011) 145, [arXiv:1003.4450].
[17] **WMAP** Collaboration, L. Page *et. al.*, *Astrophys. J. Suppl.* **170** (2007) 335, [astro-ph/0603450].
[18] M. Regis, *Astropart. Phys.* **35** (2011) 170, [arXiv:1101.5524].
[19] C. G. T. Haslam *et. al.*, *Astron. Astrophys. Suppl.* **47** (1982).
[20] K. Gorski, E. Hivon, A. Banday, B. Wandelt, F. Hansen, *et. al.*, *Astrophys. J.* **622** (2005) 759, [astro-ph/0409513].
[21] A. E. Vladimirov, S. W. Digel, G. Johannesson, P. F. Michelson, I. V. Moskalenko, *et. al.*, *Comput. Phys. Commun.* **182** (2011) 1156, [arXiv:1008.3642].
[22] A. Strong, E. Orlando, and T. Jaffe, *Astron. Astrophys.* **534** (2011) A54, [arXiv:1108.4822].
[23] D. R. Lorimer, astro-ph/030850.
[24] R. Trotta, G. Johannesson, I. Moskalenko, T. Porter, R. R. de Austri, *et. al.*, *Astrophys. J.* **729** (2011) 106, [arXiv:1011.0037].
[25] P. Mertsch and S. Sarkar, *JCAP* **06** (2013) 041, [arXiv:1304.1078].
[26] **WMAP** Collaboration, B. Gold *et. al.*, *Astrophys. J. Suppl.* **180** (2009) 265, [arXiv:0803.0715].
[27] L. La Porta, C. Burigana, W. Reich, and P. Reich, *Astron. Astrophys.* **479** (2008) 641, [arXiv:0801.0547].
[28] E. M. Berkhuijsen, C. G. T. Haslam, and C. J. Salter, *Astron. Astrophys.* **14** (1971) 252.
[29] C. J. Salter, *Bull. Astr. Soc. Ind.* **11** (1983) 1.
[30] M. Wolleben, *Astrophys. J.* **664** (2007) 349, [arXiv:0704.0276].
[31] D. A. Green, *Bull. Astr. Soc. Ind.* **37** (2009) 45.
[32] S. Sarkar, *MNRAS* **199** (1982) 97.

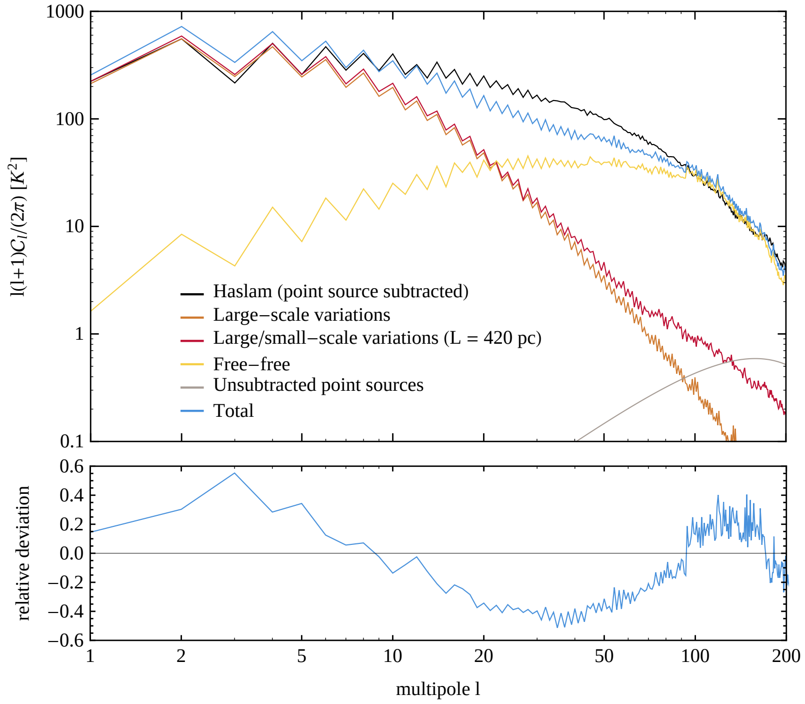

Figure 1: The angular power spectrum of the Galactic radio background: Haslam 408 MHz all-sky survey (black line), the contribution from the large-scale variation of synchrotron emissivity (red line), both large-scale and small-scale (turbulent) contributions (orange line), thermal bremsstrahlung (yellow line), unsubtracted point-sources (grey line) and the sum of all components (blue line). There is clearly a deficit in the model at $l \sim 10-100$.

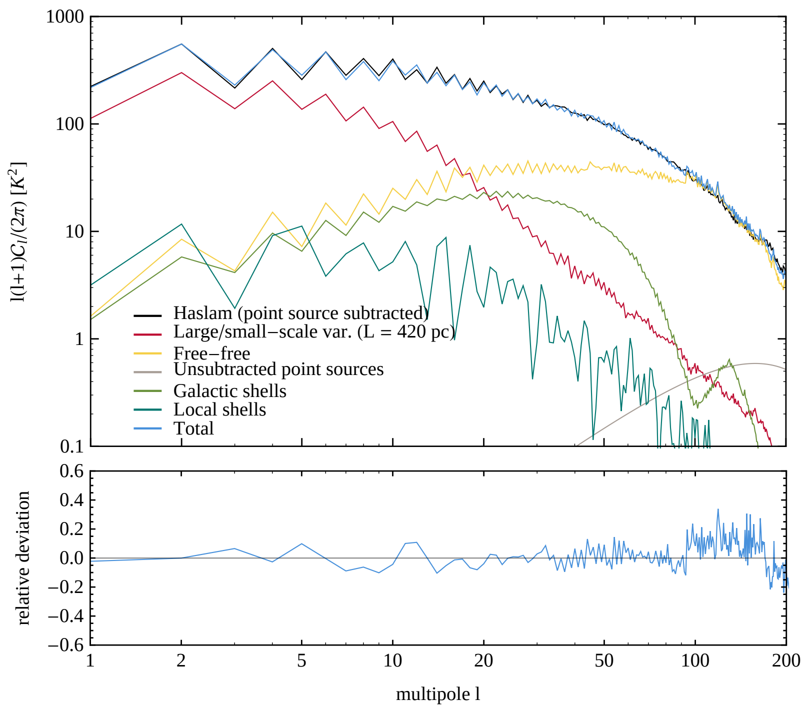

Figure 2: Same as Fig. 1, but in addition showing the contribution from the old shells of SNRs, both the Galactic population (green line) and the four local loops (green-blue line). This essentially removes the earlier deficit at $l \sim 10-100$.